



Published in final edited form as:

*Gastroenterology*. 2023 June ; 164(7): 1119–1136.e12. doi:10.1053/j.gastro.2023.01.037.

## SOX9 modulates the transformation of gastric stem cells through biased symmetric cell division

Qiyue Chen<sup>1,2,3,4,5,6,†</sup>, Kai Weng<sup>2,3,4,†</sup>, Mi Lin<sup>1,2,3,4,5,6,†</sup>, Ming Jiang<sup>7</sup>, Yinshan Fang<sup>1,6</sup>, Sanny S.W. Chung<sup>1,6</sup>, Xiaobo Huang<sup>2,3,4</sup>, Qing Zhong<sup>2,3,4</sup>, Zhiyu Liu<sup>2,3,4</sup>, Zening Huang<sup>2,3,4</sup>, Jianxian Lin<sup>2,3,4</sup>, Ping Li<sup>2,3,4</sup>, Wael El-Rifai<sup>8,9</sup>, Alexander Zaika<sup>8,9</sup>, Haiyan Li<sup>10</sup>, Anil K. Rustgi<sup>5,6</sup>, Hiroshi Nakagawa<sup>5,6</sup>, Julian A. Abrams<sup>5,6</sup>, Timothy C. Wang<sup>5,6</sup>, Chao Lu<sup>11</sup>, Changming Huang<sup>2,3,4,\*</sup>, Jianwen Que<sup>1,5,6,\*</sup>

<sup>1</sup>Columbia Center for Human Development, Department of Medicine, Vagelos College of Physicians and Surgeons, Columbia University Irving Medical Center, New York, NY 10032, USA

<sup>2</sup>Department of Gastric Surgery, Fujian Medical University Union Hospital, Fuzhou, Fujian 350001, P. R. China

<sup>3</sup>Key Laboratory of Ministry of Education of Gastrointestinal Cancer, Fujian Medical University, Fuzhou, Fujian 350001, P. R. China

<sup>4</sup>Fujian Key Laboratory of Tumor Microbiology, Fujian Medical University, Fuzhou, Fujian 350001, P. R. China

<sup>5</sup>Division of Digestive and Liver Diseases, Department of Medicine, Vagelos College of Physicians and Surgeons, Columbia University Irving Medical Center, New York, NY 10032, USA

<sup>6</sup>Herbert Irving Comprehensive Cancer Center, Vagelos College of Physicians and Surgeons, Columbia University Irving Medical Center, New York, NY 10032, USA

<sup>7</sup>National Clinical Research Center for Child Health of the Children's Hospital, Zhejiang University School of Medicine, Hangzhou, Zhejiang 310058, P.R. China

<sup>8</sup>Department of Surgery, University of Miami, Miami, FL 33136, USA

<sup>9</sup>Department of Veterans Affairs, Miami VA Healthcare System, Miami, FL 33136, USA

<sup>10</sup>Department of Pathology & Laboratory Medicine, Roswell Park Comprehensive Cancer Center, Buffalo, NY 14263, USA

\***Corresponding author:** Jianwen Que, Columbia Center for Human Development & Division of Digestive and Liver Diseases, Columbia University Irving Medical Center, NY 10032, USA, jq2240@cumc.columbia.edu, Changming Huang, Department of Gastric Surgery, Fujian Medical University Union Hospital, 32 No.29 Xinquan Road, Fuzhou 350001, Fujian, P. R. China, hcmlr2002@163.com.

**Author contributions:** QC, KW, ML, MJ, CH and JQ conceived the study, analyzed the data, and drafted the manuscript. YF analyzed scRNA-seq data. PL, SC, WR, AZ, HN, AR, AB, JA, TW and CL critically revised the manuscript for important intellectual content. ML, XH, QZ, ZL, ZH, JL and HL assisted in data collection and study design. All authors read and approved the final manuscript.

†**These authors contributed equally to this work** and should be considered co-first authors.

**Publisher's Disclaimer:** This is a PDF file of an unedited manuscript that has been accepted for publication. As a service to our customers we are providing this early version of the manuscript. The manuscript will undergo copyediting, typesetting, and review of the resulting proof before it is published in its final form. Please note that during the production process errors may be discovered which could affect the content, and all legal disclaimers that apply to the journal pertain.

**Declaration of interests:** The authors declare that they have no competing interests.

<sup>11</sup>Department of Genetics and Development, Columbia University Irving Medical Center, New York, NY 10032, USA

## Abstract

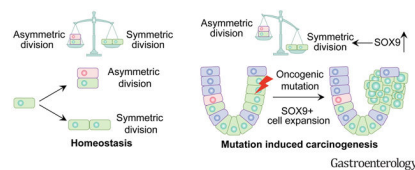
**Background and aims:** Transformation of stem/progenitor cells has been associated with tumorigenesis in multiple tissues, but in the stomach stem cells have been hard to localize. We therefore aimed to use a combination of several markers in order to better target oncogenes to gastric stem cells and understand their behavior in the initial stages of gastric tumorigenesis.

**Methods:** Mouse models of gastric metaplasia and cancer by targeting stem/progenitor cells were generated and analyzed with techniques including reanalysis of single cell RNA sequencing and immunostaining. Gastric cancer cell organoids were genetically manipulated with CRISPR/Cas9 for functional studies. Cell division was determined by BrdU chasing assay and the assessment of the orientation of the mitotic spindles. Gastric tissues from patients were examined by histopathology and immunostaining.

**Results:** Oncogenic insults lead to expansion of SOX9<sup>+</sup> progenitor cells in the mouse stomach. Genetic lineage tracing and organoid culture studies show that SOX9<sup>+</sup> gastric epithelial cells overlap with SOX2<sup>+</sup> progenitors and include stem cells that can self-renew and differentiate to generate all gastric epithelial cells. Moreover, oncogenic targeting of SOX9<sup>+</sup>SOX2<sup>+</sup> cells leads to invasive gastric cancer in our novel mouse model (*Sox2-CreERT;Sox9-loxp(66)-rtTA-T2A-Flpo-IRES-loxp(71);Kras(Frt-STOP-Frt-G12D);P53<sup>R172H</sup>*) which combines *Cre-loxp* and *Flippase-Frt* genetic recombination systems. *Sox9* deletion impedes the expansion of gastric progenitor cells and blocks neoplasia following *Kras* activation. Although *Sox9* is not required for maintaining tissue homeostasis where asymmetric division predominates, loss of *Sox9* in the setting of *Kras* activation leads to reduced symmetric cell division and effectively attenuates the *Kras*-dependent expansion of stem/progenitor cells. Similarly, *Sox9* deletion in gastric cancer organoids reduces symmetric cell division, organoid number and organoid size. In patients with gastric cancer, high levels of SOX9 are associated with recurrence and poor prognosis.

**Conclusion:** SOX9 marks gastric stem cells and modulates biased symmetric cell division, which appears to be required for the malignant transformation of gastric stem cells.

## Graphical Abstract



## Keywords

Gastric cancer; SOX2; metaplasia; neoplasia; mouse model

## Introduction

Gastric cancer (GC) is the fifth most frequently diagnosed cancer and the third leading cause of cancer death worldwide<sup>1</sup>. Despite the emergence of new surgical techniques and continued advances in chemotherapy and immunotherapy, treatment of advanced GC remains unsatisfactory. Transformation of stem/progenitor cells has been associated with tumorigenesis in multiple tissues<sup>2-5</sup>. In the intestine, deletion of adenomatous polyposis coli (*APC*) in *Lgr5*<sup>+</sup> cells leads to relatively rapid expansion of stem cells, dysplasia and eventual adenocarcinoma<sup>2</sup>. In addition, we showed that overexpression of the transcription factor *Sox2* facilitates the malignant transformation of basal stem cells in the esophagus<sup>5</sup>. By comparison, it remains largely unclear whether targeting oncogenes specifically to stem cells leads to invasive cancer in the stomach. Due to the lack of precise targeting of gastric stem cells, murine models have been limited and the cellular and molecular mechanism by which these cells are transformed remains unknown.

Gastric epithelial cells are maintained by stem cells in the isthmus where they supply progenies bi-directionally toward the top and bottom of the glands<sup>6-12</sup>. In the corpus, the gastric isthmus is located just below the gastric pits, in the upper third of the glands, while in the antrum isthmus stem cells are located close to the glandular base. These rare stem cells are marked by several proteins including *Mist1*, *Stmn1*, *Villin1*, *Bmi1*, *Lqgap3* and *eR1*<sup>6-10, 13</sup>, and in the gastric antrum also by *Cck2r*, *Aqp5* and *Lgr5*<sup>7, 11, 14, 15</sup>. The transcription factor *Sox2* is expressed in the epithelial cells of the isthmus in both the corpus and antrum. Lineage labeling studies using the *Sox2-CreERT* mouse line demonstrate tracing of all gastric lineages and thus overlap with gastric stem cells<sup>12</sup>. However, the specificity of *Sox2* and other markers for stem cells is unclear, and the isthmus also contains immature cells lacking self-renewal thought to be lineage-committed progenitor cells. Stem cells undergo both symmetric and asymmetrical division<sup>16</sup>. During homeostasis, asymmetric cell division tends to predominate giving rise to differentiated daughter cells and copies of stem cells. By contrast, increased symmetric division has been shown to promote the expansion of cancer stem cell population that drive malignant expansion<sup>17-19</sup>. Interestingly, the number of *SOX2*<sup>+</sup> cells is reduced in human GC specimens<sup>20, 21</sup>, suggesting that cancer precursors marked by other stem cell proteins likely play roles in tumorigenesis.

*SOX9* is a crucial regulator of gut development, especially for the differentiation of Paneth cells<sup>22, 23</sup>. *SOX9* is also involved in tumorigenesis and cancer progression. The increased level of *SOX9* protein has been detected in malignancies formed in multiple tissues including the mammary gland, brain, and gastro-esophageal junction<sup>24-26</sup>. Increased nuclear *SOX9* staining in esophageal malignancies is correlated with poor survival and lymph node metastasis in patients<sup>25</sup>. *SOX9* overexpression enhances tumorigenesis and promotes cancer metastasis<sup>24, 27</sup>. In the intestine, *Sox9* is expressed in the isthmus region (+4 to +7 crypt position) and lineage tracing studies using *Sox9-CreERT* mice confirmed that *Sox9* marks intestinal stem cells, with extensive lineage tracing observed both at homeostasis and after irradiation<sup>28</sup>. Moreover, increased levels of *Sox9* inhibit intestinal differentiation and promote colorectal cancer<sup>29</sup>. *SOX9* has been detected in the neck/isthmus of the corpus and antrum in human gastric samples, and the levels of *SOX9* are elevated in the gastric tissues that undergo precancerous intestinal metaplasia. Consistently, *SOX9* is highly expressed in

GC resections<sup>30</sup>. More recently, analysis of TCGA data confirmed increased SOX9 levels in GC and gastro-esophageal junctional adenocarcinomas<sup>31, 32</sup>. In line with these findings, studies with GC cell lines suggest that SOX9 inhibits apoptosis while promoting cell invasion<sup>33</sup>. Despite these studies showing the association of SOX9 with GC progression, it remains largely unknown whether this transcription factor is involved in tissue maintenance and tumorigenesis *in vivo*.

In the current study, we show that Sox9 expression is enriched in the isthmus of the corpus and antrum, and marks gastric stem cells. Lineage tracing reveals that Sox9<sup>+</sup> cells give rise to all cell lineages lining glandular units. Furthermore, some Sox9<sup>+</sup> and Sox2<sup>+</sup> cells overlap spatially. Upon specific targeting of Sox9<sup>+</sup>Sox2<sup>+</sup> cells with oncogenic mutations, invasive GCs including signet ring cell carcinoma develop in a novel mouse model, accompanied by increased Sox9 levels and symmetric cell division. Deletion of *Sox9* in Sox9<sup>+</sup>Sox2<sup>+</sup> stem cells blocks the increase in symmetric cell division and reduces the growth of GC organoids. Finally, we demonstrated that high levels of SOX9 are associated with cancer recurrence and poor prognosis in patients with GC.

## MATERIALS AND METHODS

### Mice

Mice were maintained in Columbia University's animal facility according to institutional guidelines, and all procedures were performed in accordance with the guidelines of the Institutional Animal Care and Use Committee (IACUC). To generate Sox9<sup>flippase</sup> 3'-UTR knockin mouse line, where the intact protein-coding region and endogenous expression of Sox9 were preserved, a *loxP(66)-rtTA-T2A-Flpo-IRES-loxP(71)* cassette was inserted before the stop codon of the *Sox9* gene locus by homologous recombination in embryonic stem cells. Refer to the online supplemental material for the details of other mouse lines.

### CRISPR-Cas9 system mediated SOX9 knockout

SOX9 expression was knockout in GC cells using SOX9 sgRNA CRISPR/Cas9 All-in-One Lentivector set (Human; CAT# 451541110502, Applied Biological Materials, Richmond, BC, Canada), with target sequences [CGTCGGTCATCTTCATGAAG (SOX9-CRISPR1), CGTGTCTCGGTGTCCGAGC (SOX9-CRISPR2)] and scrambled sgRNA CRISPR/Cas9 All-in-One Lentivector according to the manufacturer's instruction. In brief, plasmids (SOX9 sgRNA CRISPR/Cas9 All-in-One, scrambled sgRNA CRISPR/Cas9 All-in-One Lentivector LV053 Packaging Mix (ABM) were amplified using DH5 $\alpha$  E coli. Plasmids were transfected into HEK293T cells together with LV053 Packaging Mix (ABM) for producing viral particles using Lipofectamine 2000 (Invitrogen, Carlsbad, CA). GC cells were then infected with supernatants containing lentiviral particles in the presence of 5 ug/ml polybrene (Sigma-Aldrich, St. Louis, MO, USA). Cells with SOX9 knockout were selected by 5 $\mu$ g/ml puromycin for a week and the expression of SOX9 was evaluated by immunostaining.

## Reanalysis of single cell RNA sequencing (scRNA-seq) data

The original scRNA-seq data were generated by analyzing ~30,000 individual epithelial cells isolated from the corpus of three groups of mice (1) healthy control mice, (2) mice that have undergone acute loss of parietal cells following 3-day treatment of high-dose Tmx (5 mg/20 g body weight), and (3) *TxA23* transgenic mice that overexpress a T cell receptor specific for a peptide from H<sup>+</sup>/K<sup>+</sup>ATPase alpha chain<sup>34</sup>. Notably, the corpus of *TxA23* transgenic mice shows the loss of parietal cells, chronic inflammation, and spasmodic polypeptide-expressing metaplasia (SPEM) over a 4-month period<sup>35</sup>. FASTQ files were downloaded from NCBI (SRP227356). Cellranger v3.1.0 software (10x Genomics) was used to process FASTQ files and obtain Unique molecular identifier (UMI) counts with the GRCm38/mm10 genome as a reference. Further analysis was performed using Seurat (v3.2.1) package in R. Low-quality cells that were filtered by determining UMI counts, the numbers of transcripts and percentage of mitochondrial transcripts. `NormalizeData` and `FindVariableFeatures` functions were used for UMI counts normalization and variable features. Integration anchors were identified by `FindIntegrationAnchors` command to integrate the three groups (control, Tmx and *TxA23*), and data were integrated by `IntegrateData` command. `ScaleData` function was applied before dimensional reduction analysis. Principal component analysis (PCA) was performed, and non-linear dimensional reduction Uniform Manifold Approximation and Projection (UMAP) was applied to visualize the data. Cell clusters were identified by `FindNeighbors` and `FindClusters` functions. *Epcam* (Epithelium), *Ptpcr* (Immune), *Pecam1* (Endothelium) and *Col1a1* (Mesenchyme) were used to identify the major cell types. Epithelial cell subset was selected for re-clustering and specific cell types were identified based on the markers as previously described<sup>36</sup>.

## Tissue preparation, histology, and immunostaining

Tissues were collected and fixed in 4% paraformaldehyde overnight and processed as described previously<sup>37</sup>. Samples of mouse gastric tumors were stained with hematoxylin and eosin before evaluation by veterinary and clinical histopathologists. Immunostaining was performed according to our previously published procedures<sup>38, 39</sup>. The primary antibodies include the following: rat anti-BrdU (1:200, OBT0030, Santa BIORAD), rat anti-CD44 (1:200, 553131, BD Biosciences), rabbit anti-NUMA (1:200, NB500-174, Novus Biologicals), mouse anti-ChgA (1:500, sc-393941, Santa Cruz Biotechnology), rabbit anti-Cleaved Caspase 3 (1:500, N9664s, Cell signaling), rat anti-E-cadherin (1:200, 13-190-0, Invitrogen), rabbit anti-DCLK (1:200, ab31704, Abcam), rat anti-Sox2 (1:200, 14-9811-82, eBioscience), rabbit anti-Sox9 (1:2000, AB5535, Sigma-Aldrich), goat anti-Sox9 (1:200, AF3075, R&D Systems), mouse anti-Ki67 (1:200, 550608, BD Biosciences), mouse anti-H-K-ATPase (1:500, D032-3, MBL International), rabbit anti-GIF (1:10,000; kindly provided by D. H. Alpers, Washington University), mouse anti-MUC5AC (1:200, MS-145-P0, Lab vision), rabbit anti-GFP (1:200, A-11122, Thermofisher), goat anti-tdTomato (1:1000, orb182397, biorbyt), mouse anti-Integrin- $\alpha$ 8 (1:100, AF4076, R&D Systems), mouse anti- $\gamma$ -tubulin (1:500, T6557, MilliporeSigma), rabbit anti-Aurora B (1:200, A19539, Abclonal). For immunofluorescence, all Fluorophore-conjugated secondary antibodies were diluted to 1:500 in PBS. Griffonia simplicifolia lectin II (GSII) was detected by Alexa 488 conjugated GSII (1:500, L21415, Thermofisher). Confocal

images were obtained with a Zeiss LSM T-PMT confocal laser-scanning microscope (Carl Zeiss).

Images were viewed using Nikon SMZ1500 inverted microscope. IHC scores ranging from 0 to 9 were calculated by multiplying the intensity and expression percentage scores, expression percentage score of each sample was defined according to previous studies as: scored for the percentage of tumor cells with nuclear staining (0: no staining; 1: 1%–10%; 2: 10%–50%; and 3: >50%), and patients were categorized according to IHC scores into low (0, 1, 2 and 3) and high (4, 6 and 9) groups as previously reported<sup>32, 40, 41</sup>.

### Quantification of spindle orientation and symmetric division *in vivo*

Quantification of spindle orientation and symmetric division *in vivo* were performed similar as described previously<sup>42, 43</sup>. Late metaphase and anaphase spindles were used for the quantification. Spindles indicated by NuMA that were oriented at  $90 \pm 30^\circ$  to the basement membrane were defined as perpendicular; those that were oriented at  $0 \pm 30^\circ$  were defined as parallel. 100–200 mitoses were counted for each mouse line, which included at least three mice.

### Statistical analysis

The data were presented as the mean  $\pm$  SD. Parametric Student's t-test or nonparametric Mann-Whitney test were used for comparison of two groups, while one-way ANOVA test for multiple comparison. Kaplan-Meier analysis was used to compare survival distributions of two groups based on the log-rank test. Prognostic factors were evaluated by univariate and multivariate Cox proportional hazards models. Statistical analysis was performed using SPSS software version 22.0 (IBM Corporation Armonk, New York, USA) and GraphPad Prism version 8.0 (GraphPad Software, San Diego, California, USA), with p values indicated in the text and/or in the figures. Images of all representative histological experiments, Western blot and IF were performed at least three times independently. Statistical analysis was done using unpaired two-tailed student's t-test. Results were presented as mean  $\pm$  SD. p values < 0.05 were considered statistically significant. \*p < 0.05; \*\*p < 0.01; \*\*\*p < 0.001.

Others are described in Supplemental Materials and Methods.

## Results

### Oncogenic insults and metaplasia lead to increased numbers of Sox9<sup>+</sup> cells in the stomach of mouse models

Deletion of the Wnt signaling inhibitor *Apc* promotes the expansion of Sox2<sup>+</sup> cells and results in precancerous lesions<sup>20</sup>. We found that activation of *KRAS*, a mutated gene in GC<sup>44, 45</sup>, also led to precancerous lesion in the gastric tissues of *Sox2-CreERT;Kras(LSL-G12D)* (*Sox2Kras*) mutants. Extensive metaplasia and intraepithelial neoplasia in both antrum and corpus were observed as early as 45 days post-tamoxifen (Tmx) induction (dpi) in *Sox2Kras* mice (Figures S1A–D, S1F and S1G). By 120 dpi, multiple dysplastic lesions were detected in the gastric tissues (Figures S1B and S1E). Remarkably, Sox9<sup>+</sup>

epithelial cells were expanded in the gastric lesions. Sox9<sup>+</sup> cells were present in the normal corpus gland and were not only enriched in the isthmus of both corpus and antrum, but also overlapped with the antral base (Figures 1A and 1B). While Sox2<sup>+</sup> cells were absent from the base of the antral glands, there was strong overlap with Sox9<sup>+</sup> cells in the isthmus region. Notably, the number of Sox2<sup>+</sup> cells did not increase in *Sox2Kras* mice at 45 dpi (WT vs 45dpi: Corpus 44.9±2.6% vs. 39.7±7.4%, n=5, p=0.12; Antrum 43.8±3.5% vs 37.8±3.0%, n=5, p=0.10) (Figure 1C). By contrast, the number of Sox9<sup>+</sup> cells increased in precancerous lesions at both 45dpi and 120 dpi (Figures 1D and 1F). We then assessed Sox9<sup>+</sup> and Sox2<sup>+</sup> cells in a separate mouse model where the carcinogen N-methyl-N-nitrosourea (MNU) was used to induce GC (Figures S1H and S1I). Six of 10 wildtype C57BL6 mice developed GC following 9-month initiation treatment of MNU (Figure S1I). Consistent with the genetic model, the percentage of Sox9<sup>+</sup> cells significantly expanded (29.2±6.1% vs. 65.7±4.2%, n=6, p<0.001), while Sox2<sup>+</sup> cells did not increase in GC upon carcinogen treatment (Figures 1E and 1F). Through re-analysis of the published single cell RNA-seq data<sup>35</sup>, we found that the number of Sox9<sup>+</sup> cells also expanded in the corpus of mice treated with Tmx which induced the death of parietal cells and SPEM (Figures 1G, 1H and S2A–E)<sup>46</sup>. The expansion of Sox9<sup>+</sup> cells was also observed in *TxA23* transgenic mice that developed severe gastritis and SPEM following transgenic expression of a T cell receptor specific for a peptide from H<sup>+</sup>/K<sup>+</sup>ATPase alpha chain (Figures 1G, 1H and S2A–D). Consistently, the transcript levels of Sox9 were increased in the corpus of Tmx-treated mice and *TxA23* transgenic mice (Figure S2F). These findings confirm that Sox9<sup>+</sup> gastric epithelial cells expand following oncogenic stimulation and metaplasia. Notably, although Sox9 was enriched in isthmus progenitor cells and SPEM cells, other cell types including chief and parietal cells also express Sox9 at various levels (Figures S2E and S2G). Interestingly, Sox2<sup>+</sup>Sox9<sup>+</sup> cells were particularly enriched with the cell cycle regulatory proteins such as Cdk4 and Cdk1 (Table S1), and GO term analysis consistently demonstrated activation of cell division pathways (Table S2).

### Sox9<sup>+</sup> cells serve as stem/progenitors during homeostasis and recommit following *Kras* activation

Stem/progenitor cells in the intestine and mammary gland express Sox9<sup>27, 47</sup>. Interestingly, we noticed that 34.1±11.1% Sox9<sup>+</sup> cells were co-labeled by the proliferation marker Ki67 in the normal gastric tissue (Figure 2A). We therefore asked whether Sox9 labels stem cells in the stomach. We performed lineage tracing using *Sox9-CreERT;Rosa26<sup>TdTomato</sup>* mice. 24 hours after Tmx induction, tdTomato (tdT) expression was observed in the gastric tissues but not in the forestomach where the lining epithelium is stratified squamous (Figure 2B and data not shown). Lineage-labeled cells were first observed in the isthmus of the corpus and antrum (+4 to +7 region) and less frequently at the base of the antrum (Figure 2B). Further lineage tracing showed that the recombined cells expanded rapidly from the isthmus to trace most of the antral and corpus glands when examined at 14 dpi and the fully traced glands persisted at 180 dpi (Figure 2B). The lineage labeled cells included all cell types (e.g. parietal cells, chief, pit and enteroendocrine cells) present in the gastric tissues (Figure 2C). In addition, we isolated gastric tissues 24 hours after Tmx induction and placed them in 3D culture to determine whether lineage-labeled cells expand in organoids. Consistent with the *in vivo* data, the recombined tdT<sup>+</sup> cells expanded rapidly to populate the whole

organoids (Figure 2D). Lineage labeled cells in the organoids included the major gastric cell types such as chief and parietal cells and we also observed Sox2<sup>+</sup> and Sox9<sup>+</sup> cells (Figure S3). The dispersed organoid cells were still able to repopulate after three passages (data not shown). These data suggest that Sox9 marks gastric stem cells capable of self-renewal and differentiation.

We next generated *Sox9-CreERT;Kras(LSL-G12D)* (*Sox9Kras*) mice to test the response of Sox9<sup>+</sup> cells following oncogenic challenge. Thickened mucosa and enlarged folds were consistently observed in the corpus and antrum of *Sox9Kras* mice 120 days following *Kras* activation (Figure 2E). Introduction of *Kras* mutation led to apparent expansion of Sox9<sup>+</sup> cells (28.6±3.9% vs. 60.1±6.2%, n=4, p<0.001), among which 14.6±3.9% were co-labeled by Ki67 in mutants (Figure 2F). *Kras* activation in Sox9<sup>+</sup> cells also led to mucous metaplasia of the targeted cells as shown by the expansion of Alcian blue<sup>+</sup> cells (Corpus: 12.3±5.2% vs. 43.8±11.2%, p<0.01; Antrum: 32.8±2.9% vs. 42.2±3.5%, n=4, p<0.01) (Figure 2E). These results suggest that oncogenic mutation promotes the expansion of Sox9<sup>+</sup> progenitor cells that are associated with tissue metaplasia.

### Targeting specifically gastric Sox9<sup>+</sup> cells results in aggressive gastric cancer in a novel mouse model

The advanced tumor masses formed in the intestine prompted us to euthanize the *Sox9Kras* mice before gross tumors were fully established in the gastric tissues (Figure S4A). To circumvent the early death caused by the intestinal malignancy and obstruction, we combined the *Cre-loxp* and *Flippase (Flp)-frt* genetic recombination systems. We first established a novel knockin mouse line, where *loxp(66)-rtTA-T2A-Flp-IRES-loxp(71)* was inserted into the 3'-UTR of the *Sox9* locus (*Sox9Flp*) (Figure 3A). The transcription of *Flp* is only activated in cells that express both Cre recombinase and Sox9. We used the *Sox2-CreERT* knockin mouse line to target Cre to Sox2 lineage in the gastric isthmus. Both Sox2 and Sox9 were expressed in the mouse and human gastric isthmus (Figures 1A, 1B, S4B and S4C), where many cells expressed both markers. Our lineage tracing confirmed that Sox2<sup>+</sup> lineage encompassed Sox9<sup>+</sup> cells in mice (Figure S4D). By contrast, Sox9 but not Sox2 is expressed in the intestine (Figures S4B and S4E). To confirm the specificity of the novel *Sox9Flp* mouse line, we generated *Sox2-CreERT;Sox9Flp;Rosa26Frt-STOP-Frt-GFP* (Figure 3B). As expected, lineage labeled cells were present only in the gastric tissues when examined at 2 dpi (Figure 3C) but not in the intestine where Sox2 is absent (Figure S3F). GFP<sup>+</sup> cells were also absent in the esophagus where Sox2 was abundant but lacking Sox9 expression (Figure S4F).

*Kras* activation mutations lead to precancerous lesions (e.g. metaplasia and hyperplasia) in the mouse gastric tissue<sup>48-51</sup>. To promote cancer formation we combined *Kras* activation and p53 mutation which is commonly observed in gastric cancer<sup>50</sup>. We therefore generated *Sox2-CreERT;Sox9Flp;Kras(Frt-STOP-Frt-G12D);P53<sup>R172H</sup>* mice (*SSKP* mice) to test whether Sox9<sup>+</sup> cells serve as the cell of origin for GC (Figure 3D). Aggressive GC was detected in mutants as early as 90 dpi (Figures 3E and S5A). Invasive cancer nodules including signet ring cell carcinoma foci can also be detected in the muscle and serosal layers of the gastric wall at 150 dpi (Figures S5B and S5C). Moreover, tumor



nodules, presumably representing local metastatic spread, were present in the perigastric lymph nodes at 150 dpi (Figures 3E and S5B). Foci of cancer were also present in the liver and peritoneal at 240 dpi, again presumably representing metastases (Figures 3E and S5D). These invasive tumor phenotypes were similar to what had been observed in patients with advanced GC<sup>52, 53</sup>. As expected, no lesions were observed in the esophagus, forestomach and intestine when examined at 90 dpi (data not shown).

Persistent *Kras* and *p53* mutation activation led to the loss of differentiated gastric epithelium in SSKP mice at 90 and 150 dpi (Figure 3F). Moreover, CD44<sup>+</sup> epithelial cells were dramatically expanded, as compared to the restricted number of CD44<sup>+</sup> cells in normal control gland (3.7±1.4% vs. 75.4±2.7%, n=5, p<0.001 at 90 dpi; 4.2±1.7% vs. 95.7±1.1%, n=5, p<0.001 at 150 dpi) (Figure 3F). Our lineage tracing experiments further demonstrated these cancer cells were derived from Sox9<sup>+</sup> progenitor cells in the stomach of *SSKP;Rosa26-Frt-STOP-Frt-GFP* mice (Figure 3G). Additionally, cancer cells in the lymph node and liver also expressed GFP, implying that they were generated from the lineage labeled Sox9<sup>+</sup> cells (Figure 3H). Together our novel mouse model demonstrated that Sox9<sup>+</sup> cells serve as the cells of origin for GC in a manner that mimics human GC including signet ring adenocarcinoma.

### Sox9 is dispensable for tissue homeostasis but is essential for the initiation of gastric neoplasia

We next asked whether Sox9 is required for the maintenance of the gastric epithelium. We used *Sox2-CreER* to delete *Sox9* because SOX2 also overlaps with isthmus stem cells<sup>12</sup>. Following three doses of Tmx, Sox9 protein was not detected in the lineage-labeled gastric epithelium of *Sox2-CreERT;Sox9<sup>fl/fl</sup>;Rosa26<sup>Tdtomato</sup>* mice (Figures S6A and S6B). Lineage tracing showed that Sox2<sup>+</sup> cells generated progeny in the absence of Sox9 (Figures S6C–E). The proportion of individual differentiated cell types including enteroendocrine cells (ChgA<sup>+</sup>), tuft cells (Dclk1<sup>+</sup>), pit cells (Muc5AC<sup>+</sup>), parietal cells (HK-ATPase<sup>+</sup>) and chief cell (Gif<sup>+</sup>) remained unaltered upon *Sox9* deletion (Figure S6F). This indicates that Sox9 is not crucial for the maintenance and normal differentiation of the gastric epithelium.

We further asked whether Sox9 is required for the initiation of neoplasia originated from Sox9<sup>+</sup>Sox2<sup>+</sup> cells. We therefore generated *Sox2-CreERT;Kras(LSL-G12D);Sox9<sup>fl/fl</sup>;Rosa26<sup>Tdtomato</sup>* mice (Figure 4A). Strikingly, loss of Sox9 blocked mucous metaplasia and dysplasia, in contrast to the extensive lesions observed in *Sox2Kras* mice (Figures 4B–D, S1C and S1D). Furthermore, lineage tracing demonstrated rare tdT<sup>+</sup> cells in the gastric tissues (0–2 cells per crypt) (Figure 4B, right panel), suggesting that cells with combined *Kras* mutation and *Sox9* deletion are replaced or outcompeted by mutation-free cells. These data confirm that *Sox9* ablation reverses the gastric precancerous phenotype induced by *Kras* mutation.

We next asked whether SOX9 is also required for maintaining human GC cells. We deleted *SOX9* using the CRISPR/Cas9 recombineering in three gastric cell lines (N87, KATOIII and AGS). Loss of SOX9 protein was validated by Western blot and immunofluorescent staining (Figures S7A and S7B). We then used these cell lines to establish organoids. Deletion of *SOX9* significantly reduced the number and size of organoids initiated by the three GC cell

lines (Figures 4E–G and S7C). Upon *SOX9* deletion, the number of organoids per well in 24-well plates were significantly reduced from  $119.3 \pm 3.3$  to  $10.0 \pm 1.6$  ( $n=3$ ,  $p<0.001$ ) for the N87 cell line (91.6% reduction), from  $270.0 \pm 3.7$  to  $19.7 \pm 3.3$  ( $n=3$ ,  $p<0.001$ ) for the KATOIII cell line (92.7% reduction), and from  $141.3 \pm 3.3$  to  $26.7 \pm 1.3$  ( $n=3$ ,  $p<0.001$ ) for the AGS cell line (81.1% reduction) (Figures 4E, 4G and S7C). In addition, the sizes of the organoids established by the three GC cell lines were also dramatically reduced following *SOX9* deletion (Figures 4F and S7D). The proportion of organoids with a diameter of larger than 200  $\mu\text{m}$  was 12.0% for N87, 4.7% for KATOIII and 7.3% for AGS cells with unperturbed SOX9. By contrast, none of the three cell lines with SOX9KO formed organoids with a size larger than 200  $\mu\text{m}$  (Figure 4F). As expected, SOX9 proteins were not detected in the small organoids established by the KO cell lines (Figures 4H and S7D). Together these results illustrate that SOX9 is important for GC organoid development.

### Sox9 biases towards symmetric division in *Sox2Kras* mutants, *SSKP* mice and human gastric cancer organoids

To further explore the underlying cellular mechanisms by which Sox9 regulates tumorigenesis, we evaluated whether *Sox9* ablation affects the kinetics or turnover of the gastric epithelium. Deletion of *Sox9* had no impact on the level of apoptosis (Caspase3<sup>+</sup>) in the gastric epithelium of *Sox2Kras*; *Sox9<sup>fl/fl</sup>* mice at all time points examined (Figure S8A). Moreover, *Sox9* ablation did not cause a decrease in the proliferation (Ki67<sup>+</sup>) of Sox2<sup>+</sup> cells in the mutants (Figure S8B).

We observed an increased number of cells undergoing symmetric division in the gastric tissues of *Sox2Kras* mutants. We evaluated the type of cell division by measuring the angle between the two centrosomes formed by nuclear-mitotic apparatus protein (NuMA) and basement membrane (Integrin  $\alpha 8$ , ITGa8) (Figure S8C) as previously described<sup>54, 55</sup>. In normal gastric tissues, epithelial cells divided most frequently perpendicular to the basement membrane, indicating asymmetric division (Figure 5A). Approximately 20.2% of mitotic cells underwent symmetric division, with the remainder undergoing asymmetric cell division. By contrast, 42.7% of mitotic cells underwent symmetric division in *Sox2Kras* mice at 120dpi (Figures 5B and 5C). Furthermore, 52.5% of mitotic cells underwent symmetric division in invasive gastric adenocarcinoma of *SSKP* mutants (Figures 5B and 5C). Significantly, deletion of *Sox9* reverted symmetric division back to normal levels (20.5%) in *Sox2-CreERT;Kras(LSL-G12D);Sox9<sup>fl/fl</sup>* mutants (Figures 5B and 5C).

We next examined cell division in GC organoids by using pulse-chase BrdU labeling and paired-cell assays, as previously described<sup>19</sup> (Figure 6A). In the organoids established by the three gastric cell lines, cancer cells predominantly underwent symmetrical division as shown by equal BrdU segregation (Figures 6B–E), consistent with previous studies<sup>56</sup>. Paired-cell assays indicated that SOX9 was frequently colocalized with prelabeled BrdU (Figures 6B,6C and S9). Remarkably, ablation of *SOX9* reduced symmetric cell division in all three GC cell lines. Upon *SOX9* deletion, the cells undergoing symmetric division in the organoids were reduced from  $82.8 \pm 2.1\%$  to  $39.7 \pm 2.1\%$  ( $n=3$ ,  $p<0.001$ ) for N87 cell line, from  $89.7 \pm 2.1\%$  to  $42.0 \pm 1.6\%$  ( $n=3$ ,  $p<0.001$ ) for KATOIII, and from  $85.3 \pm 1.3\%$  to  $39.3 \pm 0.9\%$  ( $n=3$ ,  $p<0.001$ ) for AGS cell line (Figures 6D, 6E and Table S3). These

findings demonstrated that SOX9 modulates the balance between asymmetric and symmetric cell division in cancer cells. Oncogenic activation biased towards greater symmetric cell division, which appeared critical for tumorigenesis in the gastric tissues.

### **Elevated expression of SOX9 is associated with gastric cancer recurrence and poor prognosis**

In the normal human gastric corpus and antrum, SOX9<sup>+</sup> cells were mainly found in the isthmus, with only rare SOX9<sup>+</sup> cells at the base of the glands (Figure 7A). We analyzed TCGA and GEO data, and examined SOX9 expression in GC, as compared to that in corresponding normal tissues. We found that SOX9 was expressed at higher levels in GC tissues (Figure 7B). Consistent with these findings, elevated levels of SOX9 proteins were observed in GC lesions (Figures 7C and 7D). Based on immunohistochemical grading, patients were divided into low (score 0–3) and high (score 4–9) expression groups<sup>41</sup>, and more than 75% patients exhibited high levels of SOX9 regardless of the disease stages (Figures 7C and 7D). In addition, high levels of SOX9 protein were associated with an overall high recurrence rate, in particular recurrence in the liver of GC patients who had undergone curative gastrectomy (Figure 7E).

SOX9 expression levels were correlated with the overall survival rate of GC patients as revealed by Kaplan-Meier survival analysis (Figure 7F). Analysis of a tissue microarray (TMA) containing 244 GC samples showed that SOX9<sup>high</sup> patients (n=197) exhibited a poorer overall survival rate than SOX9<sup>low</sup> patients (n=47) (HR=2.51, p<0.01). SOX9<sup>high</sup> patients also showed a poor recurrence-free survival rate (HR=2.16, p<0.01) (Figure 7F). Multivariate Cox regression analysis suggested that SOX9 expression was an independent prognostic factor for the overall survival and recurrence-free survival rate (Figure 7G). We then performed stratification Kaplan-Meier analysis and asked whether SOX9 levels are associated with the prognosis of GC patients who received postoperative adjuvant chemotherapy (ACT). Both the overall survival and the recurrence-free survival rates in SOX9<sup>high</sup> patients were low regardless of receiving ACT (Figure 7H). Strikingly, SOX9<sup>low</sup> patients displayed a higher survival rate following the chemotherapy regimen recommended by the Japanese GC association (Figure 7H)<sup>52</sup>. These findings strongly imply that high levels of SOX9 protein are associated with chemotherapeutic resistance in GC patients.

### **Discussion**

Elevated Sox9 levels are associated with tumorigenesis in tissues such as the intestine and mammary gland<sup>24, 57–59</sup>. Here, we used lineage tracing and organoid culture studies to demonstrate that Sox9<sup>+</sup> gastric epithelial cells served as stem cells that are able to self-renew and differentiate into all gastric cell types. Oncogenic targeting of Sox9<sup>+</sup> cells led to highly invasive GCs developed in our novel mouse model. *Sox9* deletion impeded the expansion of gastric progenitor cells and blocked neoplasia following *Kras* activation. Further analysis revealed that *Sox9* deletion promotes asymmetric cell division in both mouse models and human GC organoids. Importantly, we showed that high levels of SOX9 are also associated with recurrence and poor prognosis in GC patients.

While the isthmus is enriched with stem cells that are critical for the maintenance and rapid repair of the gastric epithelium in both the corpus and antrum<sup>12, 60, 61</sup>, chief cells have been suggested to dedifferentiate under an injury-repair scenario<sup>62–64</sup>. In addition, the Sox2<sup>+</sup> cell lineage contains gastric stem cells<sup>12, 20</sup>. We found that a minor cell population co-expressed Sox2 and Sox9. Consistently, *Sox9-CreERT* lineage labeled cells that included all cell types in the corpus and antrum, similar to *Sox2-CreER*, indicating that the Sox9<sup>+</sup> lineage also contains gastric stem cells. Interestingly, single cell RNA-seq analysis suggests that cells co-expressing Sox2 and Sox9 are enriched with cell cycle regulatory genes. Given these observations, it seems reasonable to propose that the Sox9;Sox2 double positive cells might be the best marker for gastric stem cells that give rise to all lining epithelial cells. The Sox2<sup>-</sup>Sox9<sup>+</sup> and Sox2<sup>+</sup>Sox9<sup>-</sup> cells that are adjacent to these double positive cells might serve as progenitor cells, or could also comprise gastric stem cells needed to maintain the epithelium.

Loss of the tumor suppressor *Apc* in Sox2<sup>+</sup> stem cells leads to the formation of adenomas, but these lesions fail to progress to cancer<sup>20</sup>. Similarly, deletion of *Apc* in Lgr5<sup>+</sup> gastric stem cells also causes the formation of adenomas within a few weeks<sup>14</sup>. However, it is impossible to evaluate their potential for progression to adenocarcinoma in these models due to the rapid development of intestinal tumors that preclude longer term studies. Similarly, when we activated *Kras* in Sox9<sup>+</sup> cells using *Sox9-CreERT*, extensive intestinal tumors prompted us to euthanize the mutants before tumor progression fully developed in the gastric tissue. Our strategy that combined *Cre-loxp* and *Flp-*fl** recombination systems circumvented this issue. No tumors were observed in the intestine and esophagus of these SSKP compounds upon Tmx induction. By contrast, invasive adenocarcinoma including signet cell cancer developed in the corpus and antrum. Our strategy required the activities of both *Sox2* and *Sox9* promoters in the same cells of SSKP mice although no simultaneous activation of the two promoters is required. Thus, the cells giving rise to the invasive cancer could be Sox2;Sox9 double positive population, or Sox2-derived Sox2<sup>-</sup>Sox9<sup>+</sup> cells that could also be the cell of origin for the malignancies. It is envisioned that a combination of other promoter driven Cre or CreER with our *Sox9Flp* mouse line can target Sox9 expressing tissues/cells with high effectiveness and specificity, while simultaneously sparing the tissues/cells that express Sox9 but not Cre/CreER.

Deletion of *Sox9* using *Sox2-CreER* does not affect the proliferation and differentiation of normal gastric stem/progenitor cells. By contrast, Sox9 plays critical roles in the maintenance of intestinal stem cells, and *Sox9* deletion causes the loss of the stem cell population<sup>28</sup>. A recent study demonstrated Sox2 and Sox9 redundancy in gastric development and tumorigenesis<sup>65</sup>. However, we did not observe Sox2 overexpression and compensation for the loss of Sox9. We also did not observe increased levels of Sox2 in *Sox2-CreERT;Sox9<sup>fl/fl</sup>* and *Sox2-CreERT;Sox9<sup>fl/fl</sup>;KRAS* mouse models. Although gastric Sox9 is not essential for maintaining homeostasis, it is critical for the expansion and mucous metaplasia of Sox2<sup>+</sup> stem/progenitor cells upon *Kras* activation. *Kras* activation in Sox9<sup>+</sup> isthmus stem cells promotes mucous metaplasia, similar to previous studies where *Kras* is activated by other stem cell marker-driving CreER<sup>10, 66, 67</sup>. Deletion of *Sox9* blocks disease progression in *Sox2-CreERT;Sox9<sup>fl/fl</sup>;Rosa26<sup>Tdtomato</sup>* mutants. We further showed that loss of Sox9 biased towards normal asymmetric cell division, which effectively attenuated the expansion of stem/progenitor cells following *Kras* activation. Similarly, *SOX9*

ablation suppressed symmetric cell division, leading to the reduced size of gastric cancer organoids. Symmetric cell division, which is critical for homeostasis maintenance and tumor progression, has been postulated to be required for stem cell expansion during the earliest stages of carcinogenesis<sup>7, 17–19</sup>. Therefore, the involvement of SOX9 in the regulation of cell division could be used as a potential therapeutic target for the treatment of GC that have high levels of SOX9.

## Supplementary Material

Refer to Web version on PubMed Central for supplementary material.

## Acknowledgments:

We also thank the helpful discussion by the Que lab members. This study was supported by National Institutes of Health R01DK120650, DK100342, R01DK132251 (JQ), R01CA272901 (TW), P01CA268991 (WR), National Natural Science Foundation of China (82002462) (QC), Natural Science Foundation of Fujian Province (2020J011001) (QC), (2022J06021) (QC), Excellent Young Scholars Cultivation Project of Fujian Medical University Union Hospital (2022XH021) (QC), (2022XH041) (QC), China Scholarship Council (201908350095) (QC), (202108350068) (ML), 2R01DK114436 (HN) and P01CA098101, P30CA013696 (AR). The authors would also like to acknowledge the support by P30 DK132710, the HICCC transgenic core in part supported by P30CA013696, CCHD microscopy core supported by S10 OD032447 and FACS core supported by S10RR027050 and S10OD020056 from the NIH.

## Data availability statement

The source of mouse corpus scRNA-seq datasets was from<sup>11</sup>. FASTQ files were downloaded from NCBI (SRP227356). Any additional data are available from the corresponding authors upon request.

## References

1. Sung H, Ferlay J, Siegel RL, et al. Global cancer statistics 2020: GLOBOCAN estimates of incidence and mortality worldwide for 36 cancers in 185 countries. *CA: a cancer journal for clinicians* 2021;71:209–249. [PubMed: 33538338]
2. Barker N, Ridgway R, van Es J, et al. Crypt stem cells as the cells-of-origin of intestinal cancer. *Nature* 2009;457:608–11. [PubMed: 19092804]
3. Ang C, Hsu S, Guo F, et al. Lgr5 pericentral hepatocytes are self-maintained in normal liver regeneration and susceptible to hepatocarcinogenesis. *Proceedings of the National Academy of Sciences of the United States of America* 2019;116:19530–19540. [PubMed: 31488716]
4. Liu B, McDermott S, Khwaja S, et al. The transforming activity of Wnt effectors correlates with their ability to induce the accumulation of mammary progenitor cells. *Proceedings of the National Academy of Sciences of the United States of America* 2004;101:4158–63. [PubMed: 15020770]
5. Liu K, Jiang M, Lu Y, et al. Sox2 cooperates with inflammation-mediated Stat3 activation in the malignant transformation of foregut basal progenitor cells. *Cell stem cell* 2013;12:304–15. [PubMed: 23472872]
6. Mills JC, Shivdasani RA. Gastric epithelial stem cells. *Gastroenterology* 2011;140:412–424. [PubMed: 21144849]
7. Hayakawa Y, Nakagawa H, Rustgi AK, et al. Stem cells and origins of cancer in the upper gastrointestinal tract. *Cell Stem Cell* 2021;28:1343–1361. [PubMed: 34129814]
8. Yoshioka T, Fukuda A, Araki O, et al. Bmi1 marks gastric stem cells located in the isthmus in mice. *The Journal of Pathology* 2019;248:179–190. [PubMed: 30689202]

9. Matsuo J, Kimura S, Yamamura A, et al. Identification of stem cells in the epithelium of the stomach corpus and antrum of mice. *Gastroenterology* 2017;152:218–231. e14. [PubMed: 27670082]
10. Hayakawa Y, Ariyama H, Stancikova J, et al. Mist1 expressing gastric stem cells maintain the normal and neoplastic gastric epithelium and are supported by a perivascular stem cell niche. *Cancer cell* 2015;28:800–814. [PubMed: 26585400]
11. Hayakawa Y, Jin G, Wang H, et al. CCK2R identifies and regulates gastric antral stem cell states and carcinogenesis. *Gut* 2015;64:544–553. [PubMed: 24951258]
12. Arnold K, Sarkar A, Yram MA, et al. Sox2+ adult stem and progenitor cells are important for tissue regeneration and survival of mice. *Cell stem cell* 2011;9:317–329. [PubMed: 21982232]
13. Qiao XT, Ziel JW, McKimpson W, et al. Prospective identification of a multilineage progenitor in murine stomach epithelium. *Gastroenterology* 2007;133:1989–98. [PubMed: 18054570]
14. Barker N, Huch M, Kujala P, et al. Lgr5+ ve stem cells drive self-renewal in the stomach and build long-lived gastric units in vitro. *Cell stem cell* 2010;6:25–36. [PubMed: 20085740]
15. Tan SH, Swathi Y, Tan S, et al. AQP5 enriches for stem cells and cancer origins in the distal stomach. *Nature* 2020;578:437–443. [PubMed: 32025032]
16. Knoblich JA. Mechanisms of Asymmetric Stem Cell Division. *Cell* 2008;132:583–597. [PubMed: 18295577]
17. Chang W, Wang H, Kim W, et al. Hormonal suppression of stem cells inhibits symmetric cell division and gastric tumorigenesis. *Cell Stem Cell* 2020;26:739–754. e8. [PubMed: 32142681]
18. Sánchez-Danés A, Hannezo E, Larsimont J-C, et al. Defining the clonal dynamics leading to mouse skin tumour initiation. *Nature* 2016;536:298–303. [PubMed: 27459053]
19. Hwang W-L, Jiang J-K, Yang S-H, et al. MicroRNA-146a directs the symmetric division of Snail-dominant colorectal cancer stem cells. *Nature cell biology* 2014;16:268–280. [PubMed: 24561623]
20. Sarkar A, Huebner AJ, Sulahian R, et al. Sox2 suppresses gastric tumorigenesis in mice. *Cell reports* 2016;16:1929–1941. [PubMed: 27498859]
21. Wang S, Tie J, Wang R, et al. SOX2, a predictor of survival in gastric cancer, inhibits cell proliferation and metastasis by regulating PTEN. *Cancer letters* 2015;358:210–219. [PubMed: 25543086]
22. Mori-Akiyama Y, Van den Born M, Van Es JH, et al. SOX9 is required for the differentiation of paneth cells in the intestinal epithelium. *Gastroenterology* 2007;133:539–546. [PubMed: 17681175]
23. Bastide P, Darido C, Pannequin J, et al. Sox9 regulates cell proliferation and is required for Paneth cell differentiation in the intestinal epithelium. *The Journal of cell biology* 2007;178:635–648. [PubMed: 17698607]
24. Christin J, Wang C, Chung C, et al. Stem Cell Determinant SOX9 Promotes Lineage Plasticity and Progression in Basal-like Breast Cancer. *Cell reports* 2020;31:107742. [PubMed: 32521267]
25. Song S, Maru D, Ajani J, et al. Loss of TGF- $\beta$  adaptor  $\beta$ 2SP activates notch signaling and SOX9 expression in esophageal adenocarcinoma. *Cancer research* 2013;73:2159–69. [PubMed: 23536563]
26. Hiraoka K, Hayashi T, Kaneko R, et al. SOX9-mediated upregulation of LGR5 is important for glioblastoma tumorigenicity. *Biochemical and biophysical research communications* 2015;460:216–21. [PubMed: 25770425]
27. Guo W, Keckesova Z, Donaher JL, et al. Slug and Sox9 cooperatively determine the mammary stem cell state. *Cell* 2012;148:1015–1028. [PubMed: 22385965]
28. Roche KC, Gracz AD, Liu XF, et al. SOX9 maintains reserve stem cells and preserves radioresistance in mouse small intestine. *Gastroenterology* 2015;149:1553–1563. e10. [PubMed: 26170137]
29. Liang X, Duronio G, Yang Y, et al. An Enhancer-Driven Stem Cell-Like Program Mediated by SOX9 Blocks Intestinal Differentiation in Colorectal Cancer. *Gastroenterology* 2022;162:209–222. [PubMed: 34571027]

30. Sashikawa Kimura M, Mutoh H, Sugano K. SOX9 is expressed in normal stomach, intestinal metaplasia, and gastric carcinoma in humans. *Journal of gastroenterology* 2011;46:1292–1299. [PubMed: 21861142]
31. Zu G, Gao J, Zhou T. The Clinicopathological and Prognostic Significance of SOX9 Expression in Gastric Cancer: Meta-Analysis and TCGA Analysis. *Frontiers in oncology* 2021:3464.
32. Dong X, Song S, Li Y, et al. Loss of ARID1A activates mTOR signaling and SOX9 in gastric adenocarcinoma—rationale for targeting deficiency. *Gut* 2022;71:467–478. [PubMed: 33785559]
33. Santos JC, Carrasco-Garcia E, Garcia-Puga M, et al. SOX9 elevation acts with canonical WNT signaling to drive gastric cancer progression. *Cancer research* 2016;76:6735–6746. [PubMed: 27569216]
34. McHugh RS, Shevach EM, Margulies DH, et al. A T cell receptor transgenic model of severe, spontaneous organ-specific autoimmunity. *Eur J Immunol* 2001;31:2094–103. [PubMed: 11449363]
35. Bockerstett KA, Lewis SA, Wolf KJ, et al. Single-cell transcriptional analyses of spasmodic polypeptide-expressing metaplasia arising from acute drug injury and chronic inflammation in the stomach. *Gut* 2020;69:1027–1038. [PubMed: 31481545]
36. Ma Z, Lytle NK, Chen B, et al. Single-Cell Transcriptomics Reveals a Conserved Metaplasia Program in Pancreatic Injury. *Gastroenterology* 2022;162:604–620 e20. [PubMed: 34695382]
37. Jiang M, Ku W-Y, Zhou Z, et al. BMP-driven NRF2 activation in esophageal basal cell differentiation and eosinophilic esophagitis. *The Journal of clinical investigation* 2015;125:1557–1568. [PubMed: 25774506]
38. Que J, Luo X, Schwartz RJ, et al. Multiple roles for Sox2 in the developing and adult mouse trachea. *Development* 2009;136
39. Jiang M, Li H, Zhang Y, et al. Transitional basal cells at the squamous–columnar junction generate Barrett’s oesophagus. *Nature* 2017;550:529–533. [PubMed: 29019984]
40. Zhang D, Tang D, Rycaj K. Cancer stem cells: Regulation programs, immunological properties and immunotherapy. *Seminars in cancer biology* 2018;52:94–106. [PubMed: 29752993]
41. Wang J, Li P, Liu X, et al. An immune checkpoint score system for prognostic evaluation and adjuvant chemotherapy selection in gastric cancer. *Nature communications* 2020;11:6352.
42. Williams SE, Beronja S, Pasolli HA, et al. Asymmetric cell divisions promote Notch-dependent epidermal differentiation. *Nature* 2011;470:353–358. [PubMed: 21331036]
43. Lechler T, Fuchs E. Asymmetric cell divisions promote stratification and differentiation of mammalian skin. *Nature* 2005;437:275–280. [PubMed: 16094321]
44. Hewitt LC, Saito Y, Wang T, et al. KRAS status is related to histological phenotype in gastric cancer: results from a large multicentre study. *Gastric Cancer* 2019;22:1193–1203. [PubMed: 31111275]
45. Yeoh KG, Tan P. Mapping the genomic diaspora of gastric cancer. *Nature Reviews Cancer* 2021:1–14.
46. Saenz JB, Burclaff J, Mills JC. Modeling Murine Gastric Metaplasia Through Tamoxifen-Induced Acute Parietal Cell Loss. *Methods Mol Biol* 2016;1422:329–39. [PubMed: 27246044]
47. Furuyama K, Kawaguchi Y, Akiyama H, et al. Continuous cell supply from a Sox9-expressing progenitor zone in adult liver, exocrine pancreas and intestine. *Nature genetics* 2011;43:34–41. [PubMed: 21113154]
48. Hayakawa Y, Ariyama H, Stancikova J, et al. Mist1 Expressing Gastric Stem Cells Maintain the Normal and Neoplastic Gastric Epithelium and Are Supported by a Perivascular Stem Cell Niche. *Cancer cell* 2015;28:800–814. [PubMed: 26585400]
49. Cristescu R, Lee J, Nebozhyn M, et al. Molecular analysis of gastric cancer identifies subtypes associated with distinct clinical outcomes. *Nature medicine* 2015;21:449–56.
50. Imazeki F, Omata M, Nose H, et al. p53 gene mutations in gastric and esophageal cancers. *Gastroenterology* 1992;103:892–6. [PubMed: 1499939]
51. Seidlitz T, Chen Y, Uhlemann H, et al. Mouse Models of Human Gastric Cancer Subtypes With Stomach-Specific CreERT2-Mediated Pathway Alterations. *Gastroenterology* 2019;157:1599–1614.e2. [PubMed: 31585123]

52. Association JGC. Japanese gastric cancer treatment guidelines 2018. *Gastric cancer* 2020;24:1–21. [PubMed: 32060757]
53. Lauren P. Diffuse and so-called intestinal type carcinoma: an attempt at histological classification. *Acta Pathol Microbiol Scand* 1965;64:31–49. [PubMed: 14320675]
54. Morin X, Bellaïche Y. Mitotic spindle orientation in asymmetric and symmetric cell divisions during animal development. *Developmental cell* 2011;21:102–119. [PubMed: 21763612]
55. Larsimont J-C, Youssef KK, Sánchez-Danés A, et al. Sox9 controls self-renewal of oncogene targeted cells and links tumor initiation and invasion. *Cell stem cell* 2015;17:60–73. [PubMed: 26095047]
56. Jin G, Westphalen CB, Hayakawa Y, et al. Progastrin Stimulates Colonic Cell Proliferation via CCK2R- and  $\beta$ -Arrestin-Dependent Suppression of BMP2. *Gastroenterology* 2013;145:820. [PubMed: 23891976]
57. Jo A, Denduluri S, Zhang B, et al. The versatile functions of Sox9 in development, stem cells, and human diseases. *Genes & diseases* 2014;1:149–161. [PubMed: 25685828]
58. Lü B, Fang Y, Xu J, et al. Analysis of SOX9 expression in colorectal cancer. *American journal of clinical pathology* 2008;130:897–904. [PubMed: 19019766]
59. Blache P, Van De Wetering M, Duluc I, et al. SOX9 is an intestine crypt transcription factor, is regulated by the Wnt pathway, and represses the CDX2 and MUC2 genes. *The Journal of cell biology* 2004;166:37–47. [PubMed: 15240568]
60. Han S, Fink J, Jörg DJ, et al. Defining the identity and dynamics of adult gastric isthmus stem cells. *Cell stem cell* 2019;25:342–356. e7. [PubMed: 31422913]
61. Nienhüser H, Kim W, Malagola E, et al. Mist1+ gastric isthmus stem cells are regulated by Wnt5a and expand in response to injury and inflammation in mice. *Gut* 2021;70:654–665. [PubMed: 32709613]
62. Goldenring JR, Mills JC. Cellular Plasticity, Reprogramming, and Regeneration: Metaplasia in the Stomach and Beyond. *Gastroenterology* 2021.
63. Radyk MD, Spatz LB, Mills JC. Autophagy in cell plasticity with particular focus on paligenosis. *Autophagy in Health and Disease: Elsevier*, 2022:143–157.
64. Radyk MD, Burclaff J, Willet SG, et al. Metaplastic cells in the stomach arise, independently of stem cells, via dedifferentiation or transdifferentiation of chief cells. *Gastroenterology* 2018;154:839–843. e2. [PubMed: 29248442]
65. R F, H G, C S, et al. Gastrointestinal transcription factors drive lineage-specific developmental programs in organ specification and cancer. *Science advances* 2019;5:eaax8898. [PubMed: 31844668]
66. Kinoshita H, Hayakawa Y, Niu Z, et al. Mature gastric chief cells are not required for the development of metaplasia. *American Journal of Physiology-Gastrointestinal and Liver Physiology* 2018;314:G583–G596. [PubMed: 29345968]
67. Hata M, Kinoshita H, Hayakawa Y, et al. GPR30-Expressing gastric chief cells do not Dedifferentiate but are eliminated via PDK-Dependent cell competition during development of metaplasia. *Gastroenterology* 2020;158:1650–1666. e15. [PubMed: 32032583]



**WHAT YOU NEED TO KNOW:****BACKGROUND AND CONTEXT:**

Transformation of stem/progenitor cells has been associated with tumorigenesis in multiple tissues. By comparison, it remains largely unclear whether targeting stem/progenitor cells leads to invasive cancer in the gastric tissues.

**NEW FINDINGS:**

SOX9+ cells in the stomach are progenitor cells, capable of self-renewal and differentiation. Oncogenic targeting of SOX9+ cells causes invasive gastric cancer in a novel mouse model where a combination of Cre-Loxp and Flippase-Frt was used. Further studies reveal that Sox9 is critical for the initiation of tumorigenesis from stem/progenitor cells.

**LIMITATIONS:**

It remains to be determined how SOX9 modulates cell division at the molecular level.

**CLINICAL RESEARCH RELEVANCE:**

These data suggest that transformation of SOX9+ gastric stem cells promotes gastric tumorigenesis. They provide the basis for potentially targeting SOX9 and relevant signaling in the treatment of GC.

**BASIC RESEARCH RELEVANCE:**

Our study employed innovative mouse models to define SOX9 as a key factor and the underlying mechanism that modulates stem cell transformation, promoting tumorigenesis in the gastric tissue.

**LAY SUMMARY:**

Our study using a novel mouse model to define a key factor and the underlying mechanism that modulates the transformation of gastric progenitor cells to promote gastric tumorigenesis.

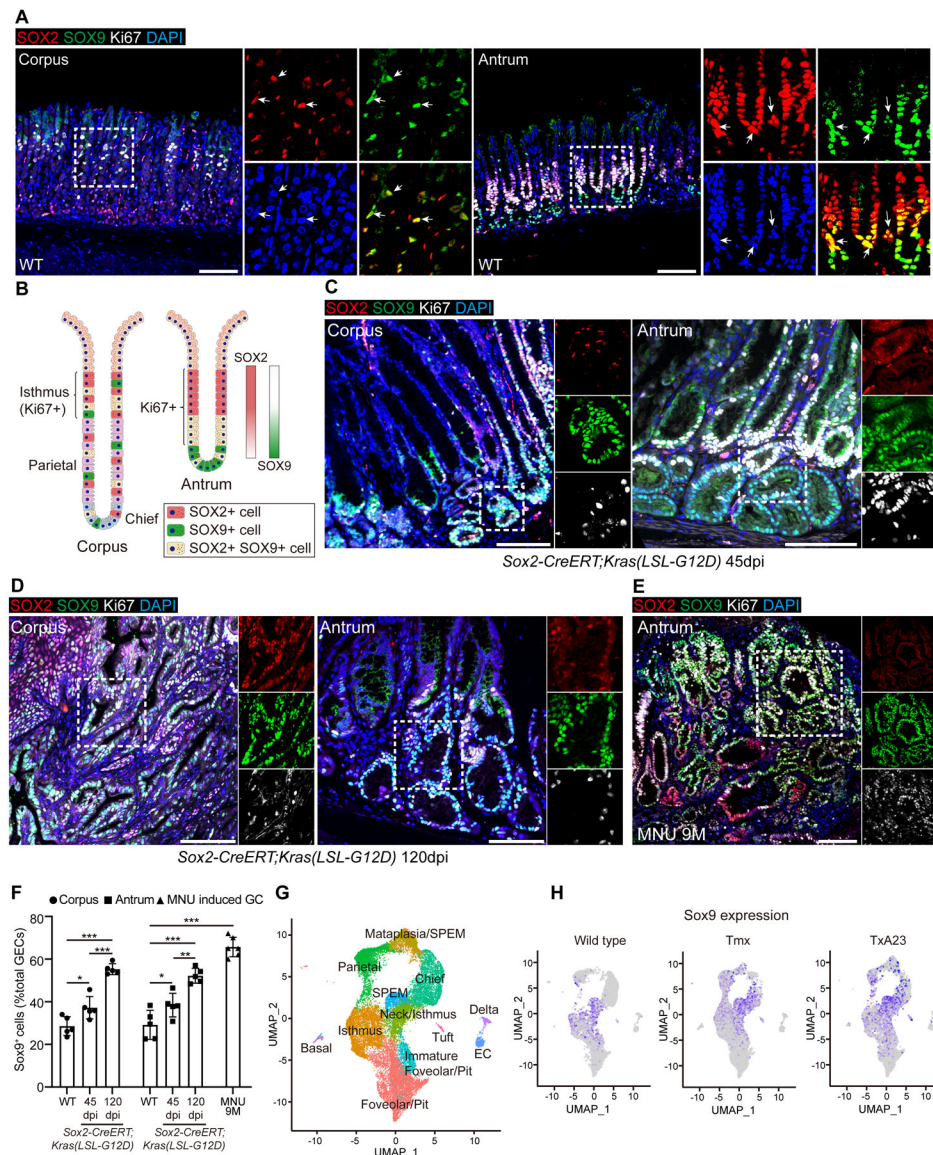


**Figure 1. Increased numbers of SOX9<sup>+</sup> cells in the stomach of SOX2-CreERT;Kras(LSL-G12D) (Sox2Kras) mice and a chemically induced gastric cancer model.**

(A) Representative images of immunofluorescence of Sox2, Sox9, Ki67 in the corpus and antrum of wildtype (WT) mice. Arrows indicate co-expression of Sox2 and Sox9. (B) Schematic depicts the expression of Sox9, Sox2 and Ki67 in the mouse stomach. (C-D) Representative images of immunofluorescence of Sox2, Sox9 and Ki67 in the corpus and antrum of *Sox2Kras* mice at different time points after tamoxifen administration. (E) Representative images of immunofluorescence of Sox2, Sox9 and Ki67 in the stomach of WT mice 9 months after MNU treatment. (F) Quantification of Sox9<sup>+</sup> cells in *Sox2Kras* mice at different time points following tamoxifen (Tmx) administration and WT mice with 9 months of MNU treatment. (G) UMAP annotation of gastric epithelial cell types from the corpus of healthy control mice, Tmx-treated mice and TxA23 transgenic mice. (H) Expression of Sox9 transcripts in the corpus of the three groups of mice as revealed by UMAP. Data are expressed as mean  $\pm$  SD. Statistical analyses used unpaired t-test or

one-way ANOVA test. \* $p < 0.05$ ; \*\* $p < 0.01$ ; \*\*\* $p < 0.001$ ; n.s. no significance. Scale bars, 100  $\mu\text{m}$ . See also Figure S1 and S2.

Author Manuscript

Author Manuscript

Author Manuscript

Author Manuscript

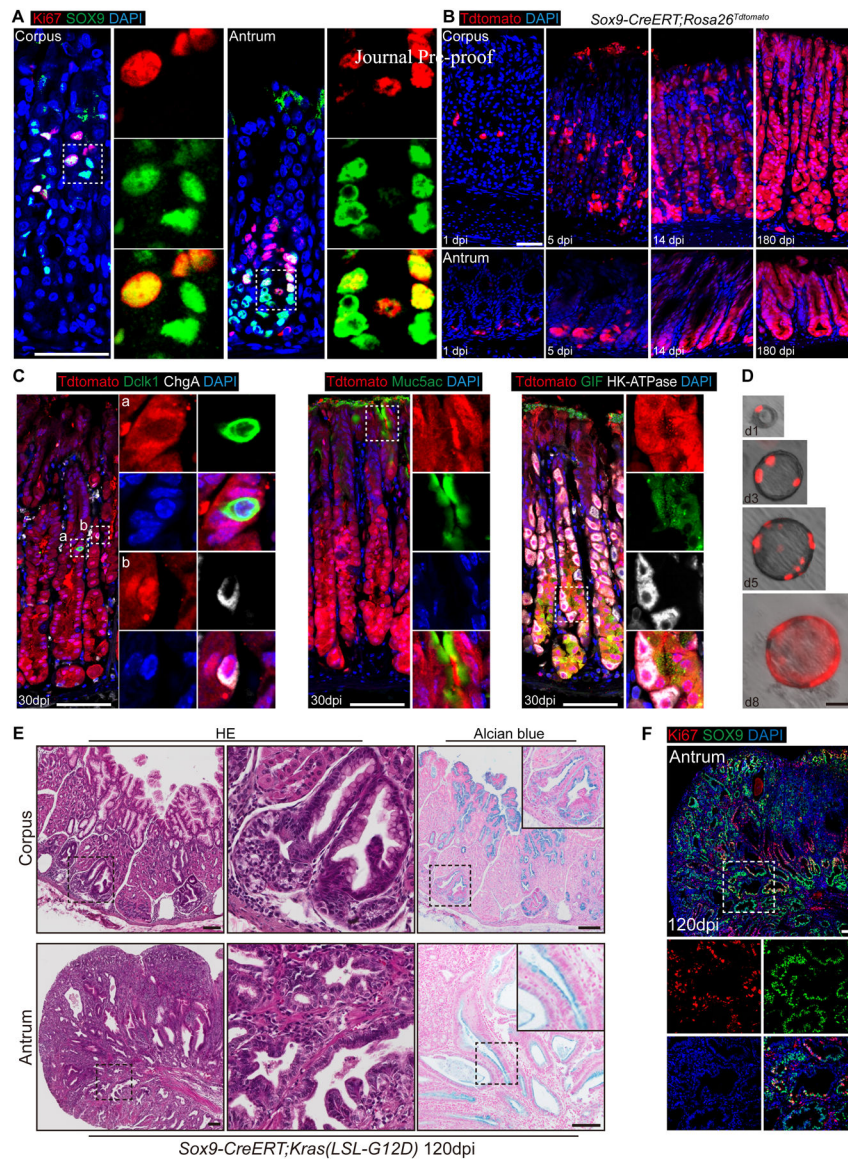


**Figure 2. Gastric Sox9<sup>+</sup> cells serve as progenitor cells during homeostasis and recommit following *Kras* activation.**

(A) Representative images of immunofluorescence of Sox9 and Ki67 in the mouse antrum and corpus. (B) Lineage-tracing in the stomach of *Sox9-CreERT; Rosa26<sup>Tdtomato</sup>* mice at different time points following a single dose of tamoxifen. (C) Staining of enteroendocrine cell (ChgA<sup>+</sup>), tuft cell (Dcl1<sup>+</sup>), pit cell (Muc5AC<sup>+</sup>), parietal cell (HK-ATPase<sup>+</sup>) and chief cell (Gif<sup>+</sup>) with Tdtomato in the stomach of *Sox9-CreERT; Rosa26<sup>Tdtomato</sup>* mice at 30 dpi. (D) Lineage tracing of gastric organoids established by using cells isolated from the gastric tissues of *Sox9-CreERT; Rosa26<sup>Tdtomato</sup>* mice 24h after Tmx induction. (E) H&E and Alcian blue staining of gastric tissues collected from *Sox9-CreERT; Kras(LSL-G12D)* mice at 120 dpi. The epithelium displays neoplasia in the corpus and dysplasia in the antrum. (F) The numbers of Sox9<sup>+</sup> cells increased in the gastric tissues of *Sox9-CreERT; Kras(LSL-G12D)* mice examined at 120 dpi. Each group has at least three mice. Scale bar in A, B, D, 50  $\mu$ m; C, E, F, 100  $\mu$ m. See also Figure S3 and S4.

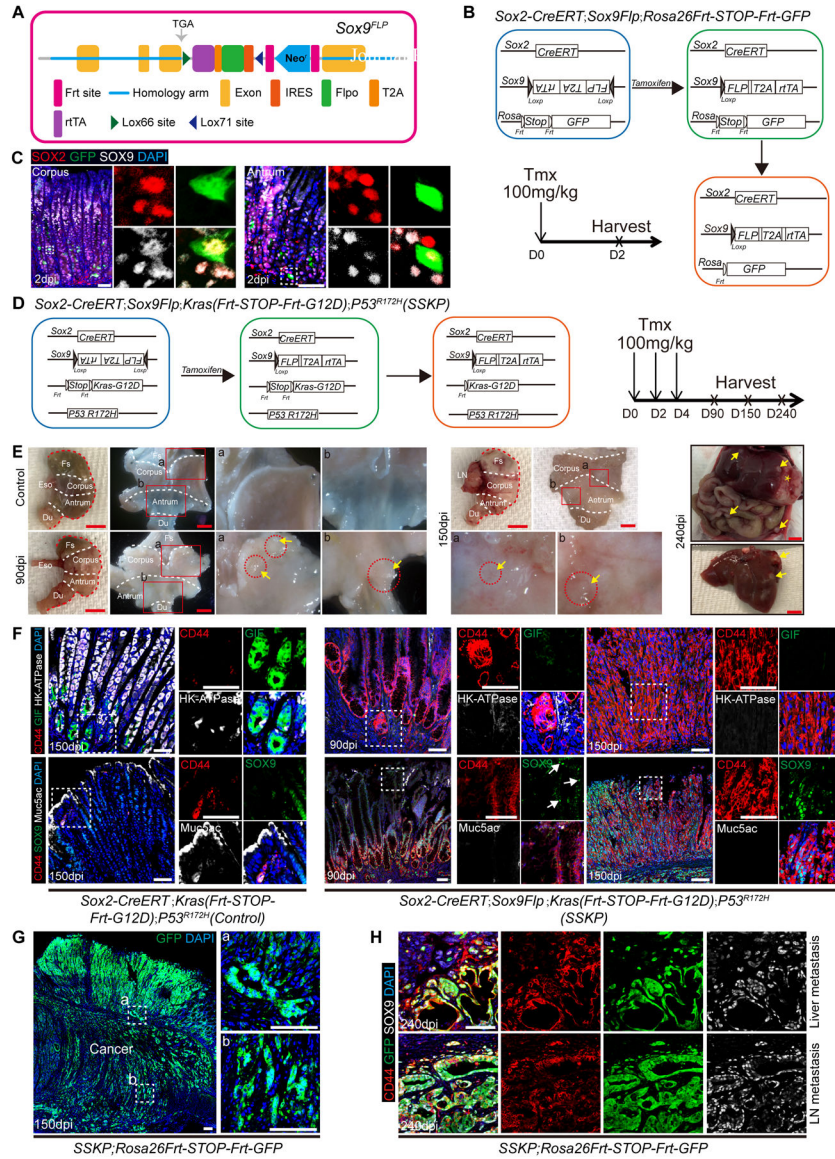


**Figure 3. Combine *Cre-loxP* and *Flpase (Flp)-Frt* system to specifically target *Sox9*<sup>+</sup> cell in the stomach.**  
 (A) Schematic depicts the knockin allele *Sox9*<sup>FLP</sup>. (B) Schematic strategy depicts the generation of *Sox2-CreERT;Sox9Flp;Rosa26Frt-STOP-Frt-GFP* mice. (C) Expression of *Sox2*, *Sox9* and *GFP* in the stomach of *Sox2-CreERT;Sox9Flp;Rosa26Frt-STOP-Frt-GFP* mice. (D) Schematic depicts the generation of *SSKP* mice. (E) Representative gross images of *SSKP* mouse stomach, liver and peritoneal metastasis at different time points after Tmx administration. Asterisks indicate primary tumor and arrows indicate metastatic tumor. (F) Expression of different cell markers in the stomach of *SSKP* and control mice at 90 and 150 dpi. Note the presence of *Sox9*<sup>+</sup> cells in the pit (arrows). (G) Lineage tracing of cancer cells in the stomach of *SSKP;Rosa26Frt-STOP-Frt-GFP* mice at 150 dpi. (H) Metastasized cancer cells express *GFP*, *CD44* and *Sox9* in the liver and lymph node of *SSKP;Rosa26Frt-STOP-Frt-GFP* mice at 240 dpi. Each group includes at least three mice. Scale bar in C, F, 50 μm; E, 5 mm; G, H, 100 μm. See also Figure S4 and S5.

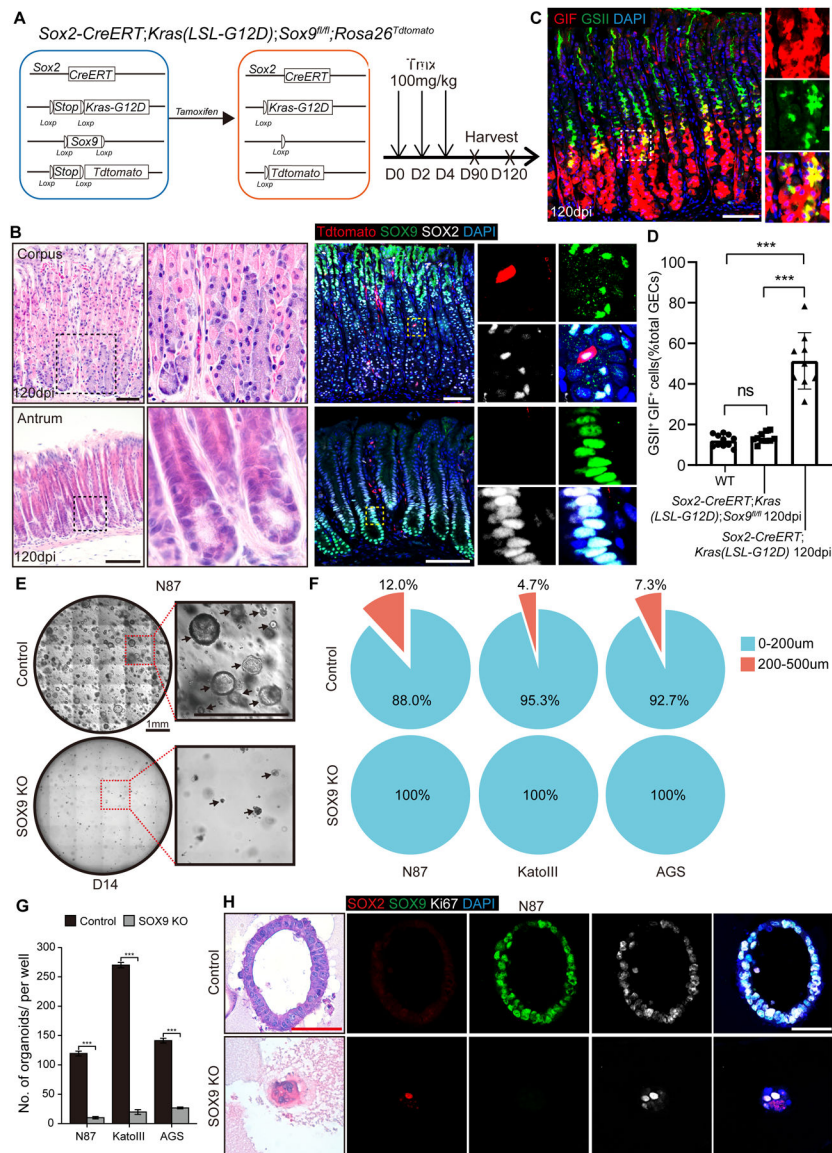


**Figure 4. Sox9 is essential for the formation of precancer lesion and gastric cancer organoid.** (A) Schematic depicts the generation of *Sox2-CreERT;Kras(LSL-G12D);Sox9<sup>fl/fl</sup>;Rosa26<sup>Tdtomato</sup>* mice. (B) H&E staining and lineage tracing in the stomach of *Sox2-CreERT;Kras(LSL-G12D);Sox9<sup>fl/fl</sup>* mice at 120 dpi. (C) Co-localization of the metaplasia markers GSII and GIF in the stomach of *Sox2-CreERT;Kras(LSL-G12D);Sox9<sup>fl/fl</sup>* mice at 120 dpi. (D) Quantification of GSII<sup>+</sup>GIF<sup>+</sup> cells in the stomach of WT, *Sox2-CreERT;Kras(LSL-G12D);Sox9<sup>fl/fl</sup>* and *Sox2-CreERT;Kras(LSL-G12D)* mice at 120 dpi (n=7 per group). (E) Organoids formed by N87 gastric cancer cells with/without *SOX9* deletion. Arrows indicate organoids. (F-G) Reduced numbers and diameters of organoids formed by gastric cancer cell lines with *SOX9* deletion. (H) H&E staining and expression of SOX2, SOX9 and Ki67 in the organoids formed by N87 gastric cancer cells with/without *SOX9*. Data are expressed as mean ± SD. Statistical analyses used unpaired t-test or one-

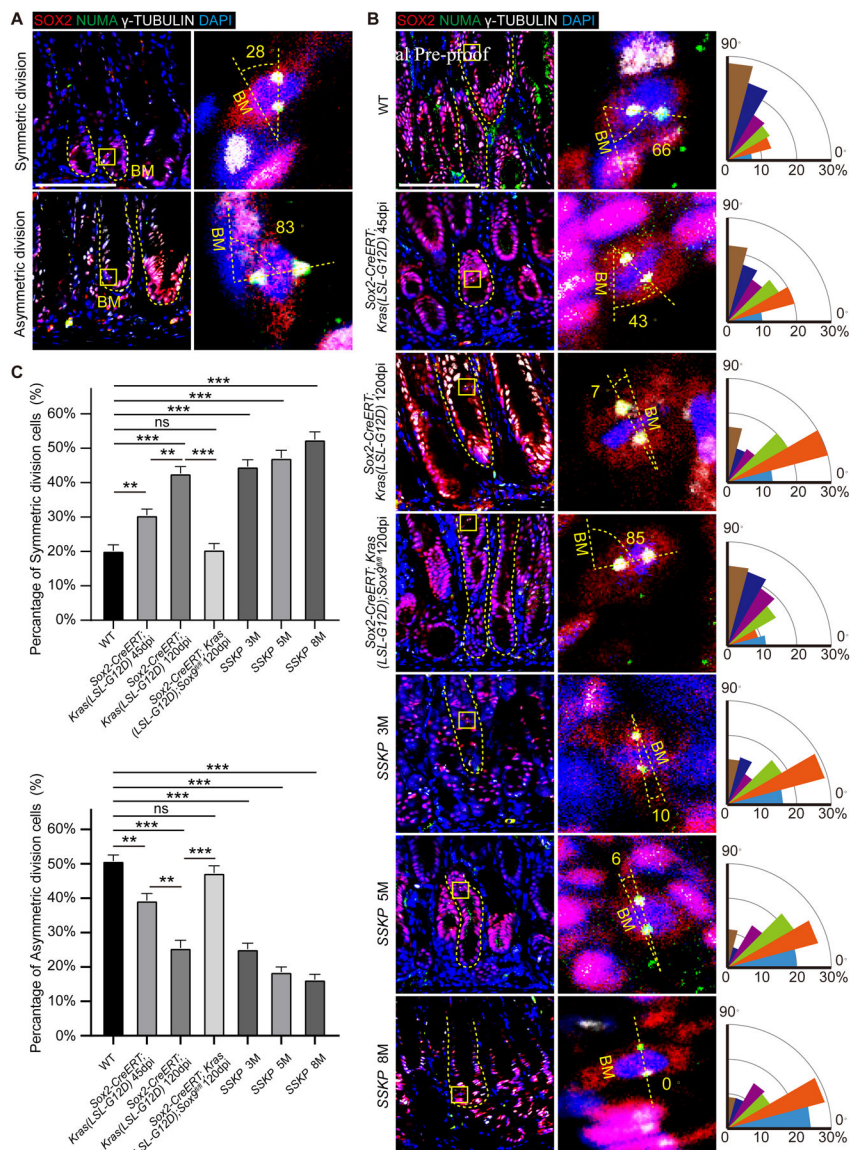
way ANOVA test. \* $p < 0.05$ ; \*\* $p < 0.01$ ; \*\*\* $p < 0.001$ ; n.s. no significance. Scale bar in B, C, 100  $\mu\text{m}$ ; E, 1 mm; H, 50  $\mu\text{m}$ . See also Figure S6 and S7.

Author Manuscript

Author Manuscript

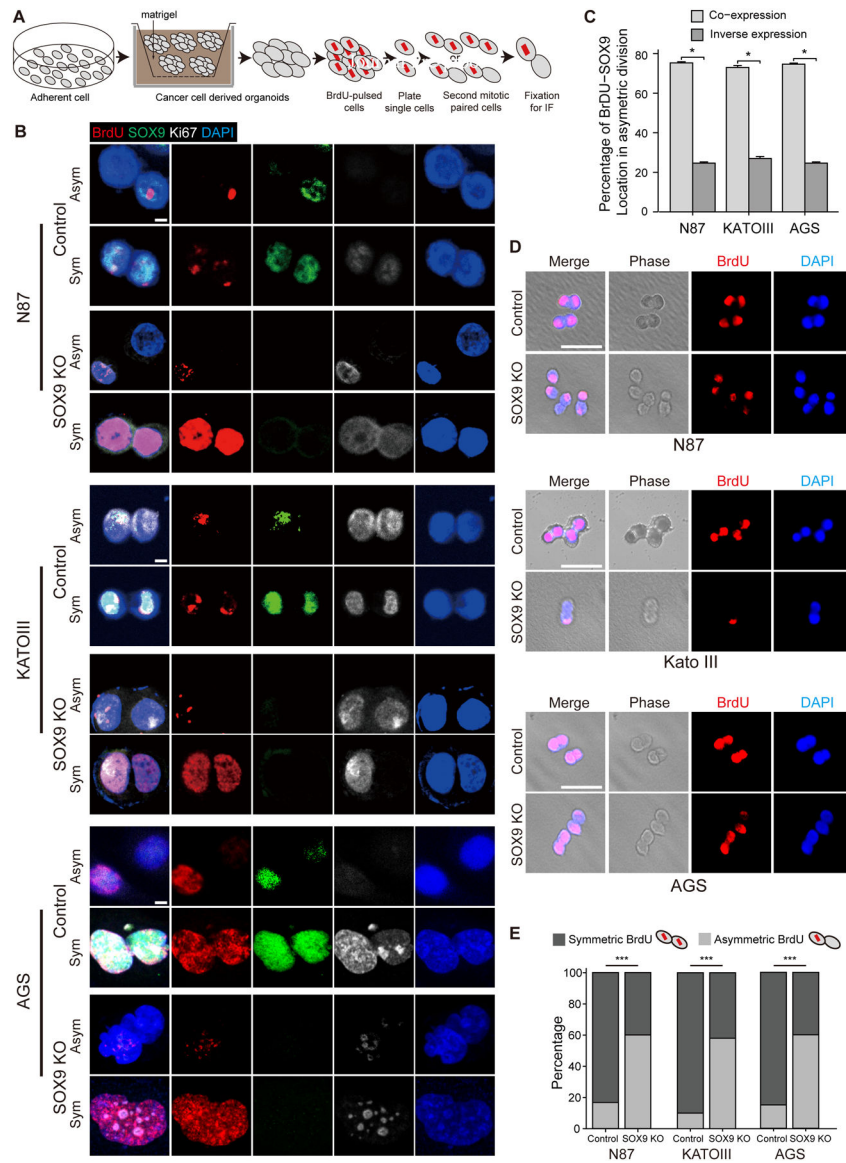
Author Manuscript

Author Manuscript



**Figure 5. Sox9 regulates symmetric division in the gastric tissues during tumor development.** (A) Epithelial cells undergo symmetrical and asymmetric division in the stomach of WT mice. Dotted line indicates the basement membrane (BM). (B) Representative images and quantification of mitotic angles of gastric epithelial cells in *Sox2-CreERT;Kras(LSL-G12D)* mutants with and without *Sox9* deletion and *SSKP* mice at different time points. (C) Quantification of symmetric and asymmetric division in B. Data are expressed as mean  $\pm$  SD. Statistical analyses used unpaired t-test or one-way ANOVA test. \* $p < 0.05$ ; \*\* $p < 0.01$ ; \*\*\* $p < 0.001$ ; n.s. no significance. Scale bar, 50  $\mu$ m. See also Figure S8.





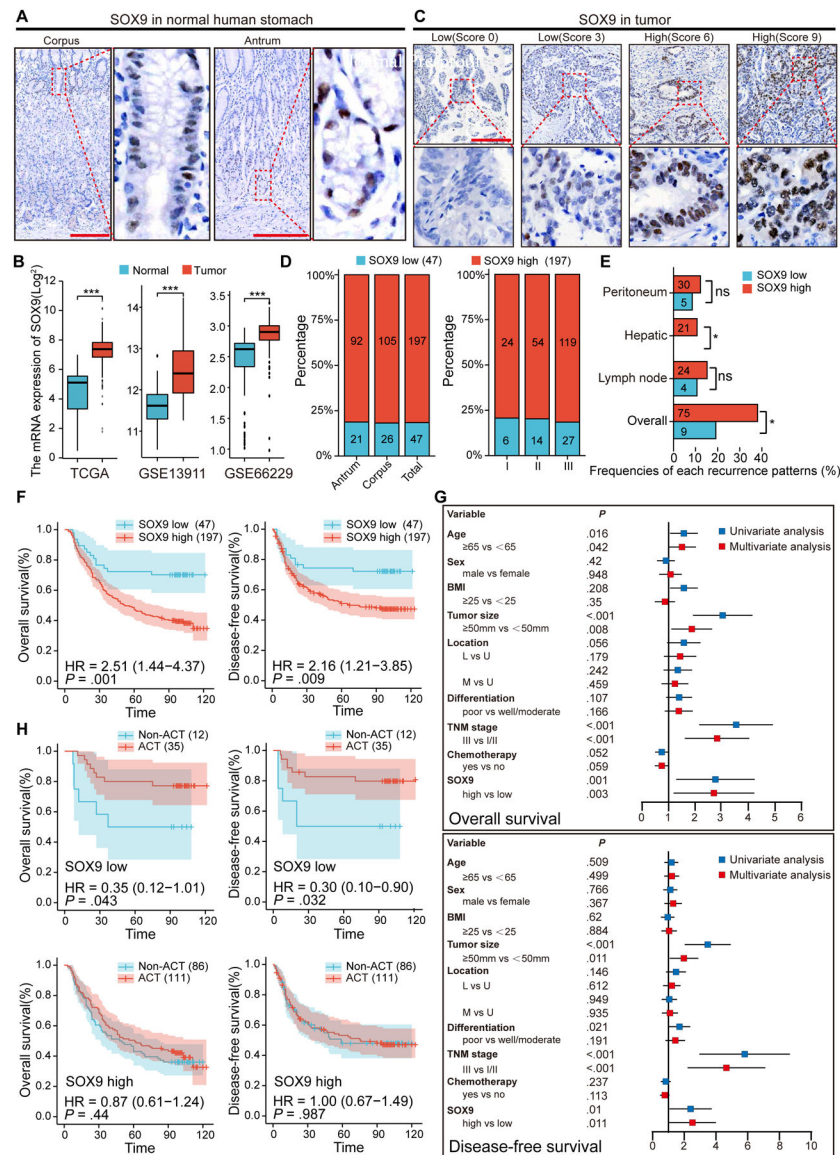


**Figure 7. Elevated expression of SOX9 is associated with gastric cancer recurrence and poor prognosis.**

(A) Representative images of SOX9 IHC staining in the normal human stomach. (B) Using TCGA and GEO database to examine the expression of SOX9 in gastric cancer and adjacent normal tissues. (C) Representative images of different score of SOX9 IHC staining in gastric cancer tissues. (D) Association of SOX9 expression, tumor location and stage in gastric cancer cohorts. (E) Association of SOX9 expression and the frequency of various recurrence patterns. (F) Kaplan-Meier analyses of the correlations between SOX9 expression and the overall survival or disease-free survival in 244 patients. (G) Univariate and multivariate survival Cox regression analyses for the 244 patients with gastric cancer. (H) Effect of chemotherapy on the overall survival and disease-free survival in gastric cancer patients with low and high SOX9 expression. ACT, adjuvant chemotherapy. Data are expressed as mean

± SD. Statistical analyses used unpaired t-test. \* $p < 0.05$ ; \*\* $p < 0.01$ ; \*\*\* $p < 0.001$ ; n.s. no significance. Scale bar in A, 200  $\mu\text{m}$ ; C, 100  $\mu\text{m}$ .